ISSN 1062-8738, Bulletin of the Russian Academy of Sciences: Physics, 2018, Vol. 82, No. 4, pp. 380–385. © Allerton Press, Inc., 2018.
Original Russian Text © P.A. Tsygankov, A.S. Skriabin, V.D. Telekh, E.Yu. Loktionov, R.Yu. Chelmodeev, 2018, published in Izvestiya Rossiiskoi Akademii Nauk, Seriya Fizicheskaya, 2018, Vol. 82, No. 4.

Interaction between Dusty Shock Waves and Three-Dimensional Scaffolds of Carbon Nanocomposites upon the Deposition of Biocompatible Coatings

P. A. Tsygankov*, A. S. Skriabin, V. D. Telekh, E. Yu. Loktionov, and R. Yu. Chelmodeev

Bauman Moscow State Technical University, Moscow, 105005 Russia

**e-mail: terra107@yandex.ru*

Abstract—The interaction between shock waves (velocity $D_0 \approx 2–2.5$ km s^{-1} and maximum pressure $p_{max} \approx 3.1–3.8$ MPa) containing finely dispersed hydroxyapatite particles (with mean diameters of $d_p \approx 70$ nm and 100 μm) and substrates of carbon nanostructured composites that are a periodic three-dimensional scaffold is investigated experimentally. Study of these processes is important for the development of nonconventional osteoconductive and biocompatible materials with properties of osteoinduction. Features of the interaction between dusty shock waves and these substrates are established on the basis of complex experimental studies. Optimum conditions and ways of forming high-adhesion coatings on carbon composites are determined.

DOI: 10.3103/S1062873818040214

INTRODUCTION

Biocompatible coatings based on stoichiometric hydroxyapatite (HA) with the formula $Ca_{10}(PO_4)_6(OH)_2$ [1] are widely used to improve the operational properties of medical implants made of various materials (metal alloys, ceramics and polymers). Typically, these coatings with characteristic thicknesses of 5–100 μm are deposited using the well-developed technologies of high-speed plasma or gas-flame powder spraying [2]. There is also the deposition of hydroxyapatite by detonative means onto ceramics [3] and titanium alloys [1]. Implants based on carbon nanocomposites, which have obvious advantages over traditionally used materials [4], are widely used in modern medical practice. A three-dimensional scaffold made of carbon rods is the basis of carbon nanostructured composite. This scaffold is filled with porous amorphized carbon that is pyrolytically precipitated and is a cementing bond of spatial construction [5, 6]. Such a composite implant allows us to reproduce the mechanical properties of both cortical and spongy bone by changing the structural parameters. It also has the properties of osteoconduction formed in the body a unique single bone–carbon block. Hydroxyapatite must be applied to the implant improve its osteoinductive properties. However, the deposition of a relatively thick coating of the HA (more than 20 μm thick) by traditional means is difficult, due to the considerable abrasive action of the powder on the porous filling and considerable stationary thermal and dynamic loads destroying the substrate. The use of high-speed flows (with characteristic velocities of $D \approx 2.0–3.5$ km s^{-1}) obtained via gas detonation [7, 8] is quite promising, due to the wide variation of the flow parameters and, most importantly, the mild action of a pulse on the substrate. At present, there is virtually no information on the interaction between dusty detonation flows and carbon composites based on three-dimensional scaffolds. As a result, such studies are of definite practical interest and relevance.

EXPERIMENTAL

The basis of our experimental setup (see Fig. 1) is CCDS 2000 unit (*1*) for detonative powder deposition [7] equipped with units for the controlled supply of fuel (*2*) (acetylene), oxygen and nitrogen, along with a system for the supply of particles (*3*) that allows the injection of 0.5–1.0 mm^3 HA perpendicular to the axis of the barrel in one working cycle. In our experiments, the original molar composition of the mixture was strictly limited by the safety requirements associated with the need for the complete oxidation of acetylene C_2H_2 to form CO_2 and H_2O, and was determined in accordance with the reaction $2C_2H_2 + 5O_2 + 7N_2 = 4CO_2 + 2H_2O + 7N_2$. Nitrogen was used to purge the installation's gas paths between working cycles. We used Puchok-M diagnostic equipment [9–11] to visualize and measure the parameters of detonation flows and shock waves.

Detonation flows were generated in a cylindrical channel/barrel with a diameter $d = 1.6$ cm after the electrical detonation of the fuel–oxidant mixture by ignition system (*4*). The proportion of channel filling

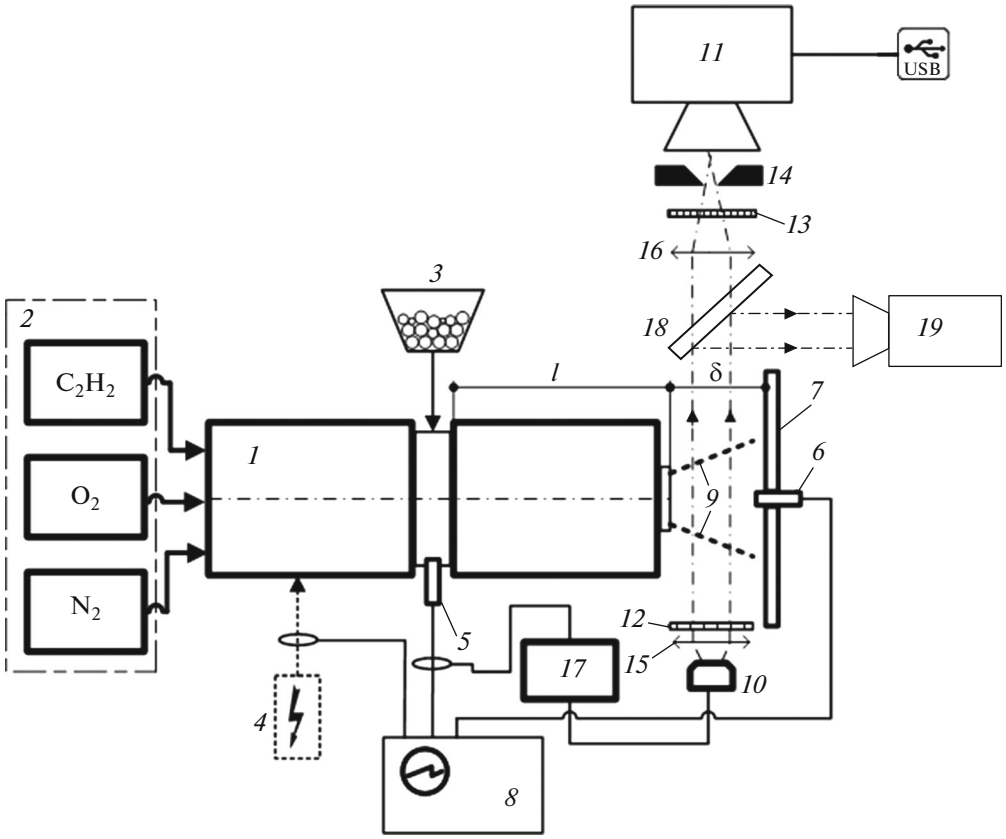

Fig. 1. Scheme of experimental stand: (*1*) the CCDS 2000 unit for detonative powder deposition; (*2*) the unit for controlled supply of fuel; (*3*) the system for feeding and supply of deposited particles; (*4*) the detonation initiation system (ignition); (*5*, *6*) piezometric pressure sensors; (*7*) a substrate; (*8*) an OWON 6062 oscilloscope; (*9*) the detonation flow; (*10*) the Nd:YAG laser (λ = 532 nm); (*11*) the camera (Videoscan-250); (*12*) a polarization filter; (*13*) an interference filter (λ_{max} = 532 and $\Delta\lambda$ = 10 nm); (*14*) a diaphragm; (*15*, *16*) lens; (*17*) the synchronizing unit, (*18*) a prism; (*19*) the Solar SC125 spectrometer.

with the fuel–oxidant mixture η was varied from 0.6 to 0.95 in our experiments. Piezometric sensors were used to measure pressure pulses. Sensor (*5*) was embedded in the barrel in the zone of particle injection, and sensor (*6*) was installed at variable distance δ from the barrel cut and mounted on fixed substrate (*7*). The δ values varied from 2.5 to 23 cm. The sensor data were recorded by a storage oscilloscope (*8*) using a synchronizing signal of ignition. The Schlieren technique was used for optical investigation of the emerging flow structures (*9*). The main nodes of this system were Nd:YAG laser (*10*) with a wavelength of 532 nm and high-speed Videoscan-250 video camera (*11*) connected via a USB interface to a computer where the image is displayed and recorded using special software. The path of the rays is shown by the arrows. Polarization filter (*12*) was used to control the intensity of the emitted laser radiation and to prevent the matrix of video camera (*11*) from incident light. Interference filter (*13*) with λ_{max} = 532 nm and $\Delta\lambda$ = 10 nm was used to reject the glow of the flux (9). Diaphragm (*14*) was installed behind this filter. Lenses (*15*) and (*16*) were used to produce a collimated laser beam and focus it on the camera lens. The delay time of the camera was set with respect to the signal from piezometric sensor (*5*) using BNC 575 synchronizing unit (*17*).

The HA particles with characteristic mean sizes of $d_p \approx$ 70 nm and 100 μm were produced by OOO Biteka. The regimes of the generation and motion of detonation flows with and without these particles were studied during our experiments.

The structure of the carbon nanocomposite used as a substrate was visualized with a Zeiss Ultra plus 55 scanning electron microscope (Fig. 2). It was a three-dimensional scaffold consisting of layered fibers connected by bonds of porous carbon. Monolithic rods with a characteristic diameter on the order of 3–5 μm were inside these fibers. Energy dispersive analysis (EDX) confirmed the chemical purity of the substrate, all elements of which consisted of carbon (99.9%). The material had high porosity, a large specific surface, and is capable of forming a highly adhesive bonds with the HA.

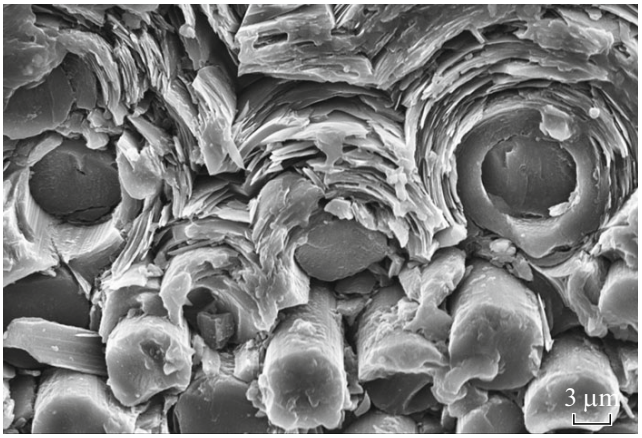

Fig. 2. Electronic photograph of the carbon nanocomposite substrate.

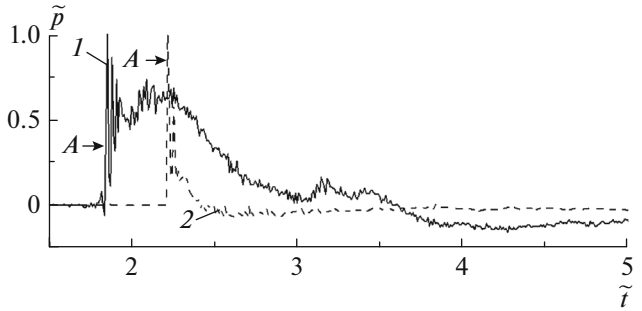

Fig. 3. Dependence of the dimensionless pressure of the impulse flow on dimensionless time when where is no HA injection and $\eta = 0.95$: (*1*) sensor in the barrel, (*2*) sensor behind the barrel cut ($\delta/d \approx 1.56$). *A* is a strong shock wave; *B* is the zone of active combustion.

RESULTS AND DISCUSSION

Our investigations allowed us to establish the main features of the interaction between detonation flows and finely dispersed HA particles, and of the formation of high-speed heterophase current. Data on the dependence of dimensionless pressure $\tilde{p} = p/p_0$ on dimensionless time $\tilde{t} = t/t_0$ in the injection zone and at a distance of $\delta = 2.5$ cm from its opening are shown in Figs. 3 and 4. These data were obtained using piezometric sensors (see Fig. 1) for the maximum filling of the barrel, $\eta = 0.95$. The characteristic pressure scale was $p_0 = 3.1$ MPa, and the characteristic time scale was $t_0 = 440$ ms.

The obtained data indicate that in all situations, strong shock wave *A* was detected by the sensor in the barrel's channel. This shock wave propagated along the unperturbed fuel–oxygen mixture with a pressure of $p_{max} \approx 3.1–3.8$ MPa and heated it to the temperatures of active combustion onset *B*. It was noted that the injection of HA particles led not only to a certain

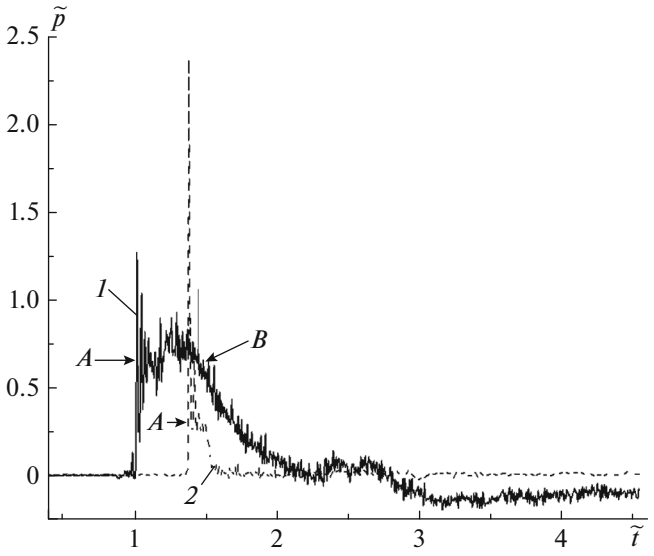

Fig. 4. Dependence of the dimensionless pressure of the impulse flow on dimensionless time when HA is injected with $d_p = 100$ μm and $\eta = 0.95$: (*1*) sensor in the barrel, (*2*) sensor behind the barrel cut ($\delta/d \approx 1.56$). *A* is a strong shock wave.

increase in $\tilde{p}_{max}$ (by approximately 1.1–1.3 times) but also increased the overall noisiness $\tilde{p}(\tilde{t})$ of the signal, due to the turbulence of the flow.

It was shown that the parameters of the shock wave detected by sensor *6* depended largely on relative distance δ/d to the substrate. The substrate was exposed to strong shock wave *A* (as in Figs. 3 and 4) with $\tilde{p}_{max} \approx$ 1.0–3.2 for relatively short δ/d (i.e., for $\delta/d < 7$). The shock wave gradually transformed into a weak wave and decayed with increasing δ/d (see Fig. 5). It was noted that the impulse detected on the substrate was higher (by approximately 1.5–3.5 times) when the HA is injected with $d_p \approx 100$ μm. This was due to the effective braking of the dispersed phase. At the same time, a sufficiently high impulse transmitted to the substrate with $\tilde{p}_{max} \approx 1.5–2.0$ was observed even when a relatively small fraction with $d_p \approx 70$ nm is used. This was because aggregations of the HA with characteristic sizes of 0.5–1.0 μm formed as a result of the coalescence of nanodispersed particles interacting with the substrate. This was confirmed through a microscopic analysis of the coating.

The mean velocity of shock waves *D* were determined at known time t_r between their registration at two points (in the barrel and at distance δ from the cut) separated by distance $l + \delta$. The maximum recorded values (for $\delta/d \approx 1.56$) were in this case $D_0 \approx$ 2.3–2.5 km s^{-1}. Figure 5 shows the attenuation dependence of dimensionless velocity $\tilde{D}(\delta/l)$, where

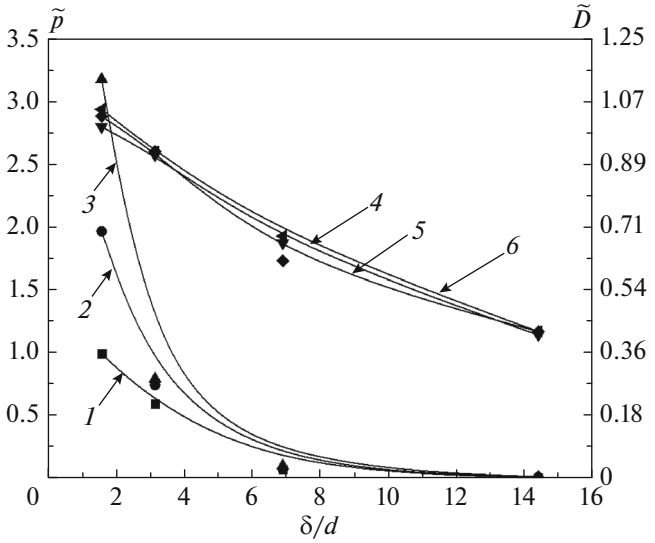

Fig. 5. Dependence of the maximum dimensionless pressure that can be recorded and the dimensionless velocity on the relative distance from the barrel cut to the substrate δ/l with $\eta = 0.95$: (*1*) without HA, (*2*) HA with d_p = 70 nm, (*3*) HA with d_p = 100 μm; (*4*) without powder, (*5*) with powder having a dispersion of d_p = 70 nm, (*6*) with powder having a dispersion of d_p = 100 μm.

$\tilde{D} = D/D_0$. It was established that the injection of the HA had virtually no effect on the velocity of the waves due to the low concentration of particles, and any variation could be explained by instability of the flow.

The Schlieren technique allowed us to establish the structure and dynamics of the flow of homo- and heterophase (with HA particles $d_p \approx 70$ nm) high-speed fluxes. No appreciable effects on the structure of the particles' shock waves at such dispersity were observed under the experimental conditions. Figure 6 shows a photo of the flow (from right to left) at a delay time of 210 μs, where we can see wave front diffraction (*1*) of a strong shock wave as it leaves barrel (*2*). Combustion zone (*3*) and turbulent mixing zone (*4*), which sucks in the surrounding gas, were detected.

The samples of coating (see Fig. 7) ≈80–100 μm thick were characterized by a homogeneous and dense structure with no visible defects. X-ray diffraction studies performed with a DRON-3M diffractometer showed that the coating was a polycrystalline hydroxyapatite in which the ratio of Ca and P concentrations was around 1.67. This corresponds to the chemical composition of the original HA, indicating that the coating was formed mainly by unevaporated HA particles when they were braked on the substrate. The evaporation and thermal decomposition of individual finely dispersed particles of hydroxyapatite could in this case also be observed.

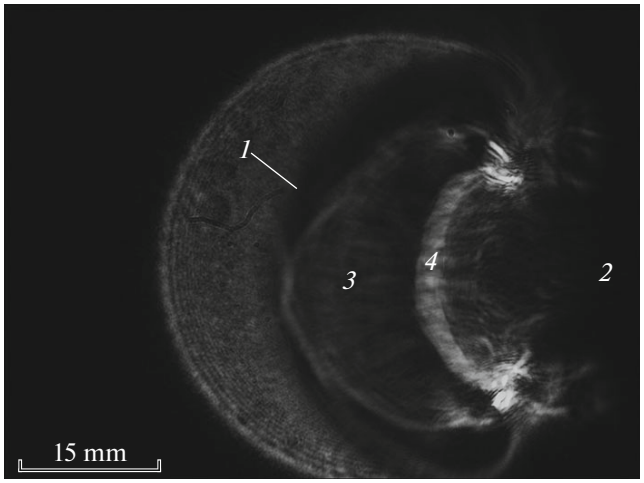

Fig. 6. Schlieren photograph of the detonation flow as it leaves the barrel (delay time, 210 μs): (*1*) the shock wave's front; (*2*) the barrel; (*3*) the region of the shocked layer; (*4*) the combustion zone.

One of the most important parameters characterizing the quality of a coating is its adhesion to the substrate. Adhesion was measured according to ISO 13779-4, as recommended in medical practice. Figure 8 illustrates the dependence of relative adhesion $\tilde{A} = A/A_{max}$ (*1*), where A_{max} is the maximum measured adhesion, along with the dependence of $\tilde{p}$ on η (*2*) at $l/d \approx 3.13$ and at an HA dispersion of $d_p \approx$ 70 nm. We can see there is an increase in relative adhesion to $\tilde{A} \approx 1$ upon raising η to $\eta \approx 0.85$ and a corresponding increase in the shock wave pressure to $\tilde{p} \approx 1$. There is then another increase in dynamic load in the carbon nanocomposite substrate upon the growth of η and $\tilde{p}$. This damages the porous carbon filling, cracking and chipping it. As a result, the adhesion of the deposited layer is reduced (to $\tilde{A} \approx 0.8$ at $\eta \approx 0.95$).

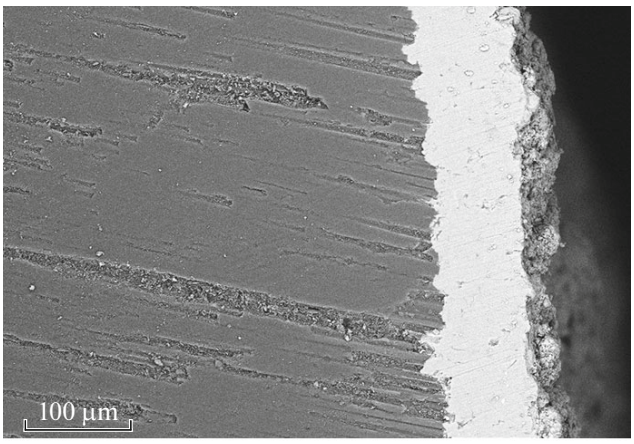

Fig. 7. Coating cross section.

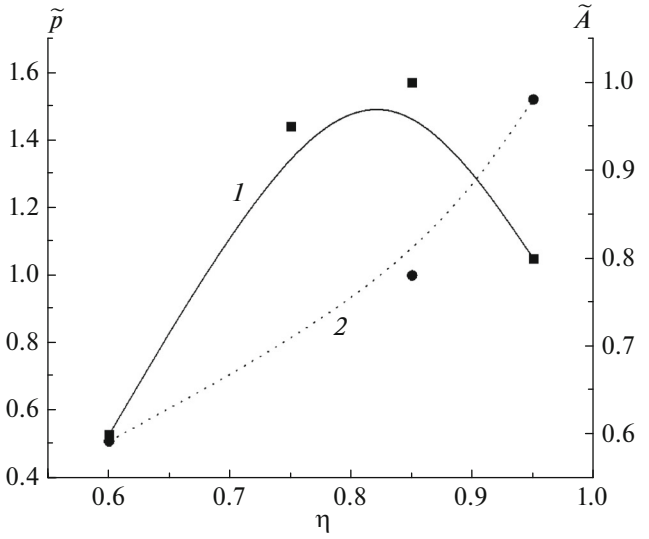

Fig. 8. Dependences of dimensionless pressure p and dimensionless adhesion A on η at $\delta/d \approx 3.13$ and upon the injection of HA particles with $d_p \approx 70$ nm: (*1*) $\tilde{A}(\eta)$ and (*2*) $\tilde{p}(\eta)$.

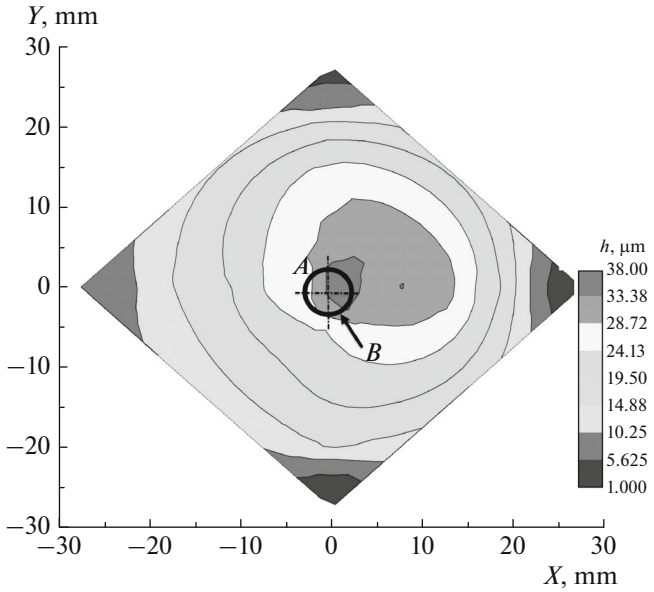

Fig. 9. Two-dimensional projection of the coating with thicknesses h, barrel position (*A*), and direction (*B*) of HA particle injection.

Following the procedure described below, we estimated how uniformly the flow was sown with particles, along with the effect this had on the homogeneity of coating. The HA coating (using particles with $d_p \approx$ 70 nm) was applied to a duralumin plate 70 × 20 × 2 mm in size using the regime parameters $\eta \approx 0.55$, $\delta =$ 18 cm, spray time $t \approx 800$ s, and response rate $n = 2$ cycles per second. The thickness of the formed coating was measured by means of stepping. Half the plate along the major axis was covered with a metallic foil 0.1 mm thick; the plate was then positioned in the holder block so that the powder hit the center piece correctly. The metallic foil was removed after treatment, and the resulting coating was examined on an FRT MicroSpy aberration profilometer. A general view of the two-dimensional projection of the coating is shown in Fig. 9. It shows the level lines corresponding to different thicknesses h of the coating, the barrel's position (*A*), and the direction of HA injection (*B*) into the barrel. We can see there is some asymmetry in the scattering of the detonation flow by particles, and thus asymmetry in the distribution of the coating's thickness, due to reflection on the inner surfaces of the barrel and the path of dosing. The maximum thickness of the resulting film was around 38.0 μm.

CONCLUSIONS

Regimes of the generation and motion of high-speed impulse flows resulting from gas detonation in a stoichiometric mixture of acetylene and oxygen, along with their mixing with finely dispersed (with $d_p \le 100$ μm) particles of HA and the formation of dusty shock waves, were investigated in this work. The time dynamics of shock wave profiles was established and the flow structure was visualized.

The morphology and adhesion of the obtained coating samples to a substrate made of carbon nanocomposites were studied. It was shown that a dense and homogeneous coating structure and maximum adhesion are observed at $l \approx 5$–6 cm and at barrel filling ratio $\eta \approx 0.8$–0.85.

ACKNOWLEDGMENTS

The unique research facility "Beam-M" used to perform these studies was supplied by the RF Ministry of Education and Science, project no. RFMEFI59014X0001. We thank OOO NanoTechMed+ for providing equipment and supporting scientific and applied research. We are grateful to V.Yu. Ul'yanitskii (Doctor of Engineering), N.S. Gavryushchenko (Doctor of Engineering) and V.A. Medik (Corresponding Member, Russian Academy of Sciences) for their advice, assistance, and discussion in performing this work.

REFERENCES

1. Nosenko, V., et al., *Nanoscale Res. Lett.*, 2015, vol. 10, p. 464.
2. Kuroda, S., Kawakita, J., Watanabe, M., and Katanoda, H., Sci. Technol. Adv. Mater., 2008, vol. 9, p. 033002.

3. Klyui, M., et al., *Funct. Mater.*, 2013, vol. 20, no. 2, p. 163.

4. Mironov, S.P., et al., *Vestn. Travmatol. Ortop. im. N.N. Priorova*, 2015, no. 3, p. 46.

5. Gordeev, S.K., et al., RF Patent 2181600, 2002.

6. Yakimenko, D.V., et al., RF Patent 2204361, 2003.

7. Nikolaev, Yu.A., Vasil'ev, A.A., and Ul'yanitskii, V.Yu., *Combust., Explos. Shock Waves*, 2003, vol. 39, no. 4, p. 382.

8. Danilenko, V.V., *Vzryv: fizika, tekhnika i tekhnologii* (Explosion: Physics, Engineering, and Technology), Moscow: Energoatomizdat, 2010.

9. Loktionov, E.Yu., Protasov, Yu.Yu., Telekh, V.D., and Khaziev, R.R., *Instrum. Exp. Tech.*, 2013, vol. 56, no. 1, p. 46.

10. Protasov, Yu.S., Protasov, Yu.Yu., Telekh, V.D., and Shchepanyuk, T.S., in *Entsiklopediya nizkotemperaturnoi plazmy* (Low-Temperature Plasma Encyclopedia), Bityurin, V.M. and Fortov, V.E., Eds., Moscow: Yanus-K, 2014, vol. IX-4, p. 388.

11. Protasov, Yu.S., Protasov, Yu.Yu., and Telekh, V.D., in *Entsiklopediya nizkotemperaturnoi plazmy* (Low-Temperature Plasma Encyclopedia), Bityurin, V.M. and Fortov, V.E., Eds., Moscow: Yanus-K, 2014, vol. IX-4, p. 452.

Translated by I. Obrezanova